Stabilization of Si60 Cage Structure

Stabilization of Si_{60} Cage Structure

Q. Sun,[1,2] Q. Wang,[1,2] P. Jena,[1] B. K. Rao,[1] and Y. Kawazoe[2]

[1]*Physics Department, Virginia Commonwealth University, Richmond, Virginia 23284-2000*
[2]*Institute for Materials Research, Tohoku University, Sendai 980-77, Japan*
(Received 13 December 2002; published 2 April 2003)

A comprehensive search for the stable geometries of bare Si_{60} and Si_{60} supported on a C_{60} fullerene was carried out using first principles calculations based on density functional theory. In contrast to previous theoretical studies and in agreement with recent experiments, we show that Si_{60} and $C_{60}@Si_{60}$ clusters are unstable in the fullerenelike cage structure. However, Si_{60} cage can be stabilized by including within it, as endohedral units, small magic clusters such as $Al_{12}X$ (X = Si, Ge, Sn, Pb) and $Ba@Si_{20}$.

Although silicon and carbon belong to the same group in the periodic table, their properties are very different. For example, the geometries of silicon and carbon clusters are not the same. In spite of numerous efforts in the past, it has not been possible to stabilize the Si_{60} cluster in the C_{60} fullerene cage structure. Harada and co-workers [1] were the first to suggest that C_{60} could be used as a reactive core onto which silicon atoms can be attached, thus forming a $C_{60}@Si_{60}$. Several theoretical studies [1–6] on the stability of $C_{60}@Si_{60}$ have since been carried out. The prediction that $C_{60}@Si_{60}$ could be energetically stable has in turn led to many experimental investigations [7–14]. Unfortunately, the observation of $C_{60}@Si_{60}$ has remained illusive [7–14]. In contrast, it has been found experimentally that Si_{60} is unlikely to wet the surface of C_{60} [12]. The puzzle, therefore, remains: how to reconcile the difference between theoretical prediction and experimental finding, and how to stabilize the Si_{60} fullerene cage? In this Letter we provide an answer to this puzzle.

We note that previous theoretical calculations [1–6] that predicted the stability of $C_{60}@Si_{60}$ had either used semiempirical methods [2–5] or did not optimize the geometry properly by relaxing it without symmetry constraint [6]. We have performed accurate first principles calculations using density functional theory [15] and generalized gradient approximation for exchange-correlation potential [16]. We find that $C_{60}@Si_{60}$ in the fullerene structure is energetically unstable and hence the inability of experimentalists to synthesize this structure is fully understandable. We further show that it is possible to stabilize Si_{60} in the cage structure by embedding magic clusters such as $Al_{12}X$ (X = Si, Ge, Sn, Pb) and $Ba@Si_{20}$ as endohedral units.

To optimize the geometry of $C_{60}@Si_{60}$ effectively and accurately, we use a plane-wave basis set with the projector-augmented wave method originally developed by Blöchl [17] and recently adapted by Kresse and Joubert in the VASP code (Vienna Ab initio Simulation Program) [18]. The structure is obtained without symmetry con-

straint and using the conjugate-gradient algorithm. We have used supercells with 14 Å vacuum spaces along x, y, and z directions for all the calculated clusters. The Γ point is used to represent the Brillouin zone due to the large supercell. The cutoff energy is taken to be 400 eV, and the convergence criteria for energy and force are 10^{-4} eV and 0.01 eV/Å, respectively. The accuracy of our method was first tested by computing the structure and properties of C_{60}. We calculate the average binding energy per atom to be 7.67 eV. The highest occupied molecular orbital (HOMO) is fivefold degenerate with h_u symmetry, and the lowest unoccupied molecular orbital (LUMO) is threefold degenerate with t_{1u} symmetry. The HOMO-LUMO gap, the longer C-C bond between a hexagon and a pentagon, and the shorter C-C bond length between the two hexagons are 1.61 eV, 1.45 Å, and 1.40 Å, respectively. These agree well with known values [19].

In order to better understand $C_{60}@Si_{60}$, we first study the structure and stability of an isolated Si_{60} cluster. In spite of considerable efforts in the past, the structure of Si_{60} is still in dispute [20]. It should be emphasized that obtaining the ground state geometry of a large cluster is not a trivial task as there are many isomers and the result may depend upon the initial geometry used for optimization. Moreover, the structures of silicon clusters are much more complicated than those of carbon. For example, the pentagon and the hexagon are the basic structural units for carbon fullerene cages. Unfortunately, for silicon clusters, such a unified picture does not exist. Many studies have been devoted to this subject and several structural models have been proposed including a fullerene cage model [20], a TTP (tricapped-trigonal-prism) model [21], and a stuffed fullerene model [22]. More important is the experimental finding of a structural transition from the elongated geometry to a more spherical one for medium sized silicon clusters [23]. To find the preferred structure of Si_{60} among the many isomers, we focus on the spherical structures as shown in Fig. 1. The first one is a fullerene cage (FC). The optimized structure
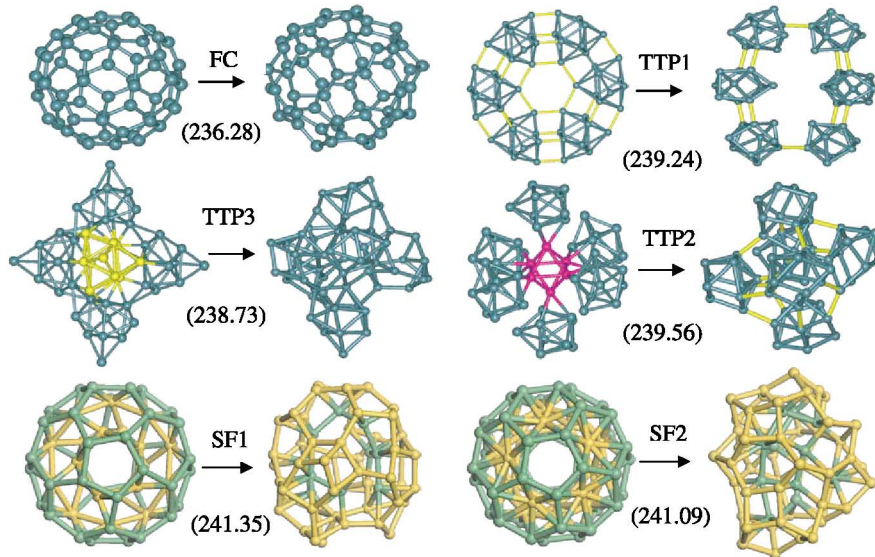
FIG. 1 (color). The starting and optimized geometries of Si_{60} obtained from fullerene cage (FC), TTP spherical stacking (TTP1-TTP3), and the stuffed fullerene type $Si_{20}@Si_{40}$ with two orientations (SF1, SF2). The numbers in parentheses show the total binding energy (eV) of the optimized structure.

has an average diameter D of 10.82 Å, a binding energy of 236.28 eV, and an energy gap of 0.59 eV. Next we consider the TTP model with three typical stacking arrays. The six $TTP-Si_{10}$ units can be arranged in a circle (TTP1), or arranged to form an octahedron with two different orientations (TTP2, TTP3). When optimized, the octahedral skeletons remain and the energies are lower than that of the FC structure. Finally we consider the stuffed fullerene (SF) structure that can also result in a spherical-like geometry. The well-known stuffed fullerene structure for silicon clusters is Si_{33} [22] in which the tetrahedral core of Si_5 is encapsulated into a Si_{28} fullerene cage. For Si_{60}, we consider Si_{20} encapsulated into Si_{40}, both having the fullerene structures. Note that C_{20} is the smallest fullerene with dodecahedral geometry [24], while the stable structure for C_{40} has D_{5d} symmetry [25] that matches the C_{20} cage. The different relative orientations give two higher symmetric structures with symmetry of C_5 and S_{10} for $Si_{20}@Si_{40}$. These are shown in Fig. 1 and labeled as SF1 and SF2, respectively. When fully optimized, the geometries are distorted, and the SF1 derived structure is more spherical in shape and more stable in energy than the SF2 derived structure.

Although there is no guarantee that the SF1 structure is, after optimization, the ground state geometry for Si_{60}, we can make the following conclusions: (i) Si_{60} with a fullerene cage structure is not stable energetically, in contrast to previous findings [20]. (ii) TTP structure is not the building block for Si_{60}. (iii) For medium sized silicon clusters, the spherical structure is more stable and is in agreement with experiment [23].

Next we study the stability of C_{60} encapsulated in Si_{60}. In the initial geometry, both C_{60} and Si_{60} have the I_h symmetry. However, due to the covalent bonding features of Si and C atoms, the interactions between these two cages should be orientation dependent. Here we consider three initial configurations. In the first one, C_{60} and Si_{60}

have the same orientation, as shown in Fig. 2(a) (labeled as configuration $R0$). Rotating the Si_{60} cluster by 30° relative to C_{60} around the sixfold axis, we get configuration $R6$ [Fig. 2(b)]. Similarly, rotating the Si_{60} cluster by 30° relative to C_{60} around the fivefold axis, we get configuration $R5$ [Fig. 2(c)]. When fully optimized, the $R5$ and $R6$ derived configurations have similar energies but different energy gaps. The structure derived from $R0$ is found to be more stable than those derived from $R6$ and $R5$ with an energy difference of about 1.2 eV. In all three cases, after optimization, silicon cages are severely distorted and some bonds are broken. The average diameter of the silicon cage increases to 11.03, 11.11, and 11.05 Å for $R0$, $R6$, and $R5$ derived structures,
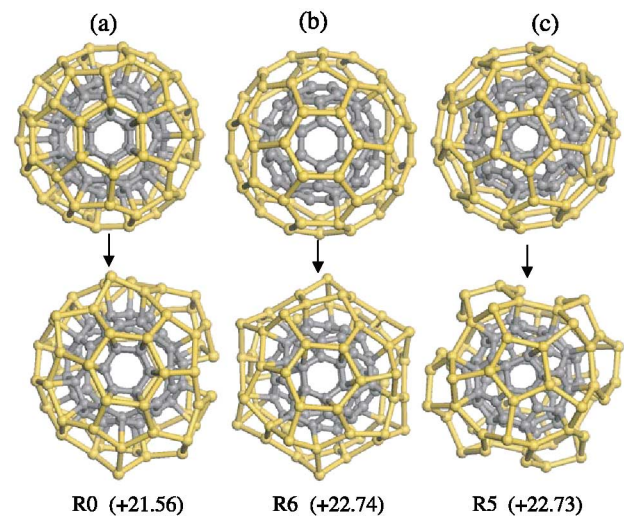

FIG. 2 (color). Equilibrium geometries of $C_{60}@Si_{60}$ obtained from symmetry unrestricted optimization of three different initial configurations (a) $R0$, (b) $R6$, and (c) $R5$. The numbers in parentheses are the encapsulating energies (in eV) of C_{60} into Si_{60} with respect to SF1.

TABLE I. Data for $C_{60}@Si_{60}$. E is the total binding energy (in eV); D_{Si60} and D_{C60} are the average diameters; R_{Si-Si}, R_{C-C}, and R_{Si-C} are the average bond lengths (in Å); and Δ is the encapsulating energies calculated using the reference energy of Si_{60} with SF1 geometry.

Cluster	E	Gap	D_{Si60}	R_{Si-Si}	D_{C60}	R_{C-C}	R_{Si-C}	Δ
C_{60}	460.29	1.61			6.945	1.434		
Si_{60} (FC)	236.28	0.59	10.82	2.28				
Si_{60} (SF1)	241.35	0.37	10.68	2.30				
$C_{60}@S_{60}$ (R0)	680.08	0.45	11.03	2.45	7.10	1.43	2.03	+21.56
$C_{60}@S_{60}$ (R6)	678.90	0.19	11.11	2.47	6.98	1.44	2.05	+22.74
$C_{60}@Si_{60}$ (R5)	678.92	0.43	11.05	2.43	6.99	1.44	2.04	+22.72

respectively, as shown in Table I. We define the encapsulation energy as the energy difference between compound cage $C_{60}@Si_{60}$ and the separated cages, i.e., $\Delta = E(C_{60}@Si_{60})$-$E(C_{60})$-$E(Si_{60})$.

Using the energy of the SF1 derived structure of Si_{60} in Fig. 1 as the reference, we find Δ to be +21.56, +22.74, and +22.73 eV for $R0$, $R6$, and $R5$ derived structures (Fig. 2), respectively. These are very large energies indeed. This suggests that $C_{60}@Si_{60}$ is unstable energetically, and Si_{60} is unlikely to wet C_{60}. This is in agreement with experiment [12] and this is why $C_{60}@Si_{60}$ cannot be successfully synthesized [7–14]. The main reason for the instability of $C_{60}@Si_{60}$ is that C_{60} is a large cluster and it stretches the Si-Si bonds in order to be accommodated as an endohedral complex. The Si-C bonding is not strong enough to compensate for the energy cost of stretching the Si-Si bonds.

We now investigate alternative ways of stabilizing Si_{60} in the cage structure. Recently several studies have been performed on small silicon cages by doping metal atoms. These include $W@Si_{12}$ [26,27], $Cr@Si_{12}$ [28], $M@Si_{15}$ (M: 3d transition element) [29], and $M@Si_{20}$ ($M =$ Ba, Sr, Ca, Zr, Pb) [30]. It is expected that a metal atom of suitable size can provide effective bonding to compensate for the energy loss that may arise from the change in the interatomic distances of the silicon atoms. Si_{20} is found to

be the largest cage that can be stabilized by doping one metal atom [30]. To stabilize the Si_{60} cage, one metal atom may not be enough. Thus we have considered stable metal clusters as endohedral complexes. This choice is guided by two important requirements: (1) We choose a metal cluster that is intrinsically very stable, namely, a magic cluster. (2) We want the geometry of this embedded cluster to share structural characteristics with the fullerene cage. We note that the fullerene geometry of a 60-atom cage consists of 12 pentagons and 20 hexagons. A 13-atom icosahedric cluster containing 12 metal atoms, which are situated along axes passing through the centers of the 12 pentagons, can conform to the structural symmetry of the fullerene. This is shown in Fig. 3(a). On the other hand, placing 20 atoms on the axes passing through the centers of 20 hexagonal rings will correspond to a dodecahedron. This is shown in Fig. 3(b). For the former case, the good candidates for the doped clusters are $Al_{12}Ge$, $Al_{12}Sn$, $Al_{12}Pb$, and $Al_{12}Si$, which are icosahedric clusters. They correspond to 40-electron systems that were predicted to be suitable building blocks of cluster assembled materials [31] and they have been identified in the recent experiments as stable clusters [32]. The diameters for these clusters are around 5.3 Å. Note that the sum of the radii of the silicon and aluminum atoms is about 2.5 Å. Therefore, as a rough estimate, the
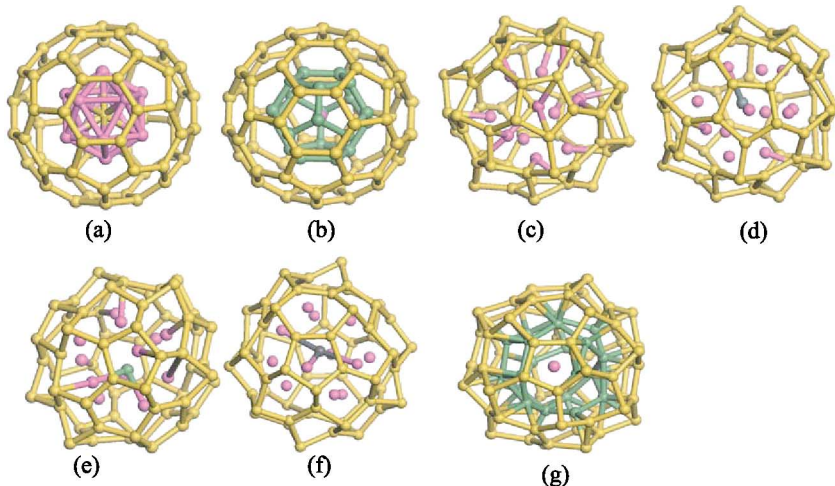

FIG. 3 (color). The initial configuration of (a) Si_{60} encapsulating icosahedral clusters $Al_{12}X$ and (b) Si_{60} encapsulating $BaSi_{20}$ dodecahedron cluster. The optimized geometries of (c) $Al_{12}Si@Si_{60}$, (d) $Al_{12}Ge@Si_{60}$, (e) $Al_{12}Sn@Si_{60}$, (f) $Al_{12}Pb@Si_{60}$, and (g) $BaSi_{20}@Si_{60}$.

TABLE II. Energetics and interatomic distance of $Al_{12}X@Si_{60}$ ($X = $ Si, Ge, Sn, Pb) and $BaSi_{20}@Si_{60}$. E is the total binding energy (in eV), and Δ is the encapsulating energies (in eV) calculated using the reference energy of Si_{60} with SF1 geometry. D_{Si60} and R_{Si-Si} are, respectively, the average diameter and the average bond length for the outer-Si_{60} shell (in Å), and R_{s-c} is the average distance between the outer shell and the inner core (in Å).

Cluster	E	Gap	D_{Si60}	R_{Si-Si}	R_{s-c}	Δ
$Al_{12}Si@Si_{60}$	287.81	0.21	10.48	2.34	2.67	-9.53
$Al_{12}Ge@Si_{60}$	287.66	0.29	10.68	2.34	2.71	-10.66
$Al_{12}Sn@Si_{60}$	287.73	0.22	10.91	2.44	2.72	-11.69
$Al_{12}Pb@Si_{60}$	287.38	0.23	10.90	2.44	2.72	-12.72
$BaSi_{20}@Si_{60}$	327.87	0.29	10.83	2.41	2.40	-14.15

space left in $Al_{12}X@Si_{60}$ would be good for the bonding between Al atoms and Si cage, as confirmed in our calculations. For the embedded cluster with a dodecahedral structure, we have chosen $Ba@Si_{20}$ [30], which is also stable and has a diameter of 6.7 Å that is intermediate between those of C_{60} and C_{20}. The calculated data are listed in Table II. In all these cases, the encapsulating energies are negative, so the compound cages are stable in energy. Meanwhile the silicon cage bond length and the cage diameters are smaller than those in the $C_{60}@Si_{60}$ case. Because of the strong interaction of aluminum atoms with the silicon cage, the embedded clusters of $Al_{12}X$ ($X = $ Si, Ge, Sn, Pb) are all decomposed but they remain encapsulated, as shown in Figs. 3(c)–3(f). These magic clusters do not display magic behavior when interacting with the silicon cage. This is consistent with the fact that the bond strength (2.38 eV) in the AlSi dimer is much stronger than that of Al_2 (1.38 eV) [33]. Figure 3(g) shows the optimized geometry of $BaSi_{20}@Si_{60}$ with an encapsulating energy of -14.15 eV.

In summary, detailed calculations are performed on $C_{60}@Si_{60}$ which is found to be energetically unfavorable. This explains the recent experimental observation that Si_{60} is unlikely to wet the C_{60} surface. However, it is possible to stabilize Si_{60} as a cage structure if one uses smaller magic clusters such as $Al_{12}X$ ($X = $ Si, Ge, Sn, Pb) and $Ba@Si_{20}$ as endohedral units. These clusters have geometries that are commensurate with the fullerene structure and can be embedded without causing too much strain in the Si-Si bonds. The accuracy of the theoretical method is high enough for us to predict that synthesis of Si_{60} in the fullerene structure is possible if one uses small metal clusters as endohedral complexes. We await experimental verification of our prediction.

[1] M. Harada *et al.*, Chem. Lett. **1**, 1037 (1994).
[2] S. Osawa *et al.*, Fullerene Sci. Technol. **3**, 225 (1995).
[3] D. E. Jemmis, J. Leszczynski, and E. Osawa, Fullerene Sci. Technol. **6**, 271 (1998).
[4] E. F. Sheka *et al.*, Int. J. Quantum Chem. **88**, 441 (2002).
[5] H. Tanaka *et al.*, J. Phys. Chem. B **103**, 5939 (1999).
[6] X. G. Gong and Q. Q. Zheng, Phys. Rev. B **52**, 4756 (1995).
[7] T. Kimura, T. Sugai, and H. Shinohara, Chem. Phys. Lett. **256**, 269 (1996).
[8] M. Pellarin *et al.*, Chem. Phys. Lett. **277**, 96 (1997).
[9] C. Ray *et al.*, Phys. Rev. Lett. **80**, 5365 (1998).
[10] M. Pellarin *et al.*, J. Chem. Phys. **110**, 6927 (1999).
[11] M. Pellarin *et al.*, Eur. Phys. J. D **9**, 49 (1999).
[12] M. Pellarin *et al.*, J. Chem. Phys. **112**, 8436 (2000).
[13] M. Ohara *et al.*, J. Phys. Chem. A **106**, 4498 (2002).
[14] F. Tournus *et al.*, Phys. Rev. B **65**, 165417 (2002).
[15] W. Kohn and L. Sham, Phys. Rev. **140**, A1133 (1965).
[16] J. P. Perdew *et al.*, Phys. Rev. B **46**, 6671 (1992).
[17] P. Blöchl, Phys. Rev. B **50**, 17 953 (1994).
[18] G. Kresse and D. Joubert, Phys. Rev. B **59**, 1758 (1999); G. Kresse and J. Hafner, Phys. Rev. B **48**, 13 115 (1993).
[19] P. W. Fowler *et al.*, *An Atlas of Fullerenes* (Oxford, New York, 1995).
[20] B. X. Li, P. L. Cao, and D. L. Que, Phys. Rev. B **61**, 1685 (2000), and references therein.
[21] J. Müller *et al.*, Phys. Rev. Lett. **85**, 1666 (2000).
[22] E. Kaxiras, Phys. Rev. Lett. **64**, 551 (1990).
[23] R. R. Hudgins, M. Imai, and M. F. Jarrold, J. Chem. Phys. **111**, 7865 (1999).
[24] M. F. Jarrold, Nature (London) **407**, 26 (2000).
[25] X. Yang *et al.*, Phys. Chem. Chem. Phys. **4**, 2546 (2002).
[26] H. Hiura, T. Miyazaki, and T. Kanayama, Phys. Rev. Lett. **86**, 1733 (2001).
[27] Q. Sun, Q. Wang, Y. Kawazoe, and P. Jena, Phys. Rev. B **66**, 245425 (2002).
[28] S. N. Khanna, B. K. Rao, and P. Jena, Phys. Rev. Lett. **89**, 016803 (2002).
[29] V. Kumar and Y. Kawazoe, Phys. Rev. Lett. **87**, 045503 (2001).
[30] Q. Sun *et al.*, Phys. Rev. B **65**, 235417 (2002).
[31] S. N. Khanna and P. Jena, Phys. Rev. Lett. **69**, 1664 (1992).
[32] X. Li and L-S Wang, Phys. Rev. B **65**, 153404 (2002).
[33] *Handbook of Chemistry and Physics*, edited by D. R. Lide (CRC Press, Boca Raton, 1993), 74th ed., pp. 9–51.